Materials Today Bio 29 (2024) 101337

Contents lists available at ScienceDirect

Materials Today Bio

journal homepage: www.journals.elsevier.com/materials-today-bio

Injectable microgels containing genetically engineered bacteria for colon cancer therapy through programmed Chemokine expression

Yazhou Chen [a,b,*,1], Kehan Cai [a,1], Hui Zhao [c], Wenshuai Li [b], Xiaofang Gao [c], Yinzheng Fu [c], Kyubae Lee [e], SiTian Li [d,**], Shengjie Yao [c,***], Tao Chen [b,****]

[a] The First Affiliated Hospital of Zhengzhou University, Zhengzhou University, Zhengzhou, Henan, 450052, PR China
[b] Henan Institute of Advanced Technology, Zhengzhou University, Zhengzhou, Henan, 450003, PR China
[c] Zhengzhou Revogene Technology Co., LTD, Airport District, Zhengzhou, Henan, 451162, PR China
[d] School of Biomedical Engineering, Shenzhen Campus of Sun Yat-sen University, Guangming District, Shenzhen, Guangdong, 518107, PR China
[e] Department of Medical Engineering, College of Medicine, Yonsei University, Seoul, 03722, Republic of Korea

ARTICLE INFO

Keywords:
Chemokines
Genetically engineered bacteria
Soluble expression
Cancer immunotherapy
Microspheres
Bacteria-based therapy

ABSTRACT

Chemokines are emerging as important targets for cancer immunotherapy due to their role in regulating immune cell migration and activation within the tumor microenvironment. Effective delivery and sustained presence of chemokines at the tumor site is essential for recruiting and activating immune cells to exert anti-tumor effects. In this study, we report a genetically engineered bacterial cell factory designed for the continuous production of chemokine CCL21 in a controlled manner. To decrease the formation of infusion bodies (IBs) in bacteria, we used thioredoxin (Trx) as the fusion partner and cloned at N-terminal of the target protein. The commonly used promoters, pT7-LacO, pBV220, and pDawn, were employed to explore the influence of various inducers on the expression of CCL21 in bacteria. The engineered bacteria were finally encapsulated within spherical gelatin methacryloyl (GelMA) microgels, which not only maintained bacterial viability but also prolonged their retention in the intestines of mice. As a result, the sustained presence and localized production of CCL21 led to effective suppression of tumor growth.

1. Introduction

Chemokines, acting as chemotactic cytokines, play a pivotal role in recruitment of immune cells [1,2]. Due to their intricate and expansive structures, chemokines offer high specificity and activity, making them promising candidates to enhance the effectiveness of cancer immunotherapy [3,4]. Despite their advantages, challenges like low stability, short half-life, and poor tissue penetration have limited the direct therapeutic application of chemokines [5,6]. Overcoming these obstacles is imperative to fully harnessing their therapeutic potential.

In recent years, bacteria have been extensively studied due to their capability to selectively target and impede tumor growth, and some of the bacterial species have undergone engineering processes to facilitate the delivery of protein drugs. This approach not only overcomes the challenges of low stability and short half-life associated with protein drugs but also enhances their therapeutic efficacy by precisely delivering them to the intended target, thereby minimizing off-target effects and reducing systemic toxicity [7]. The concept of bacteria-mediated cancer therapy dates back to the 19th century, marking its early exploitation in medical research [8]. Interest in bacteria-mediated cancer therapy has been reignited in the late 20th and early 21st centuries as researchers begin to better understand the complex interactions between the immune system, bacteria, and cancer [9–11]. Currently, employing genetic engineering to transform bacteria into functional microrobots represents a common strategy aimed at enhancing delivery efficiency and therapeutic efficacy [12–14]. Genetically engineered bacteria possess the ability to sense various environmental cues such as chemical components like L-arabinose [15], isopropyl

* Corresponding author. The First Affiliated Hospital of Zhengzhou University, Zhengzhou University, Zhengzhou, Henan, 450052, PR China.
** Corresponding author.
*** Corresponding author.
**** Corresponding author.
E-mail addresses: yzchenbio@zzu.edu.cn (Y. Chen), lisitian@gs.zzu.edu.cn (S. Li), sjyao1986@163.com (S. Yao), zzuchentao@yahoo.com (T. Chen).
[1] The authors contributed equally to this work.

https://doi.org/10.1016/j.mtbio.2024.101337
Received 25 July 2024; Received in revised form 26 October 2024; Accepted 9 November 2024
Available online 13 November 2024

β-D-1-thiogalactopyranoside (IPTG) [16], light [17,18] or temperature [19]. Leveraging this capability, the microrobots can be programmed to synthesize and release therapeutic components (eg., IFN-γ [20], NDH-2 [12], and CD47 nanoantibody [21]). The bacteria and their byproducts are named live biotherapeutic products (LBPs) [22]. Generally, LBPs can offer a cost-effective alternative to the expensive manufacturing of therapeutic protein drugs. Moreover, the localized production of protein drugs at tumor sites can significantly reduce the side effects associated with conventional protein drug delivery. However, the formation of infusion bodies (IBs) in bacteria has become one of the most reported events when using these microbial cell factories to produce functional recombinant protein drugs, particularly the proteins of eukaryotic origin [23,24]. IBs typically arise from misfolded proteins, which are often deemed as waste products [25]. Hence, converting this inactive and insoluble proteins into soluble and correctly folded products is an area of great interest.

Chemokine receptor 7 (CCR7) is a G protein-coupled receptor comprising seven transmembrane domains. It is expressed on various cell types including central memory T cells, regulatory T cells, immature/mature dendritic cells (DCs), natural killer cells, and a minority of tumor cells [26–28]. Chemokine ligand 21 (CCL21) serves as the high-affinity ligand for CCR7, initiating cell migration within tissues [29]. The interaction between CCR7 and CCL21 plays a crucial role in promoting the migration of immune cells towards tumors, thereby facilitating immune surveillance and potentially boosting anti-tumor immune responses. However, the expression of CCR7 on tumor cells can likewise facilitate their migration towards lymph nodes, thus promoting metastasis and evading immune detection. Consequently, the establishment of a microenvironment rich in CCL21 becomes essential for the success of cancer immune therapy, aiming to enhance anti-tumor immune responses effectively. In our recent study, we successfully produced recombinant CCL21 chemokines using a prokaryotic expression system with a fused thioredoxin (Trx) tag. Our findings indicate that the resulting recombinant chemokine, Trx-CCL21, holds potential as a viable candidate for creating a CCL21-rich microenvironment conducive to tumor cells [16]. Expanding upon this groundwork, our objective is to explore the utilization of the CCL21 expression system as a bacteria-based therapeutic platform for the treatment of malignant tumors. In this study, we designed and employed commonly used promoters, namely pT7-LacO, pBV220, and pDawn, to investigate the impact of various inducers on the expression of CCL21 in Bacteria (Scheme 1). Additionally, we cloned the fusion partner thioredoxin (Trx) at the N-terminal of the target protein to examine whether the Trx partner could influence their solubility during expression.

The genetically engineered bacteria were then encapsulated in gelatin methacryloyl (GelMA) microgels to fabricate microspheres (Bac@Mic), effectively creating a bacterial cell factory. The obtained Bac@Mic exhibits a notable capacity for recruiting CCR7 positive cells. Moreover, it significantly prolongs the residence time in the intestine of mice, thus enabling the localized production of CCL21. Consequently, this study aims to formulate and refine effective therapeutic strategies centered around the delivery of CCL21 for cancer therapy.

2. Materials and methods

2.1. Materials

Ampicillin, kanamycin and isopropyl-β-D-thiogalactopyranoside (IPTG) were purchased from Beyotime Biotechnology (Shanghai, China). Protein molecular weight marker and loading buffer were

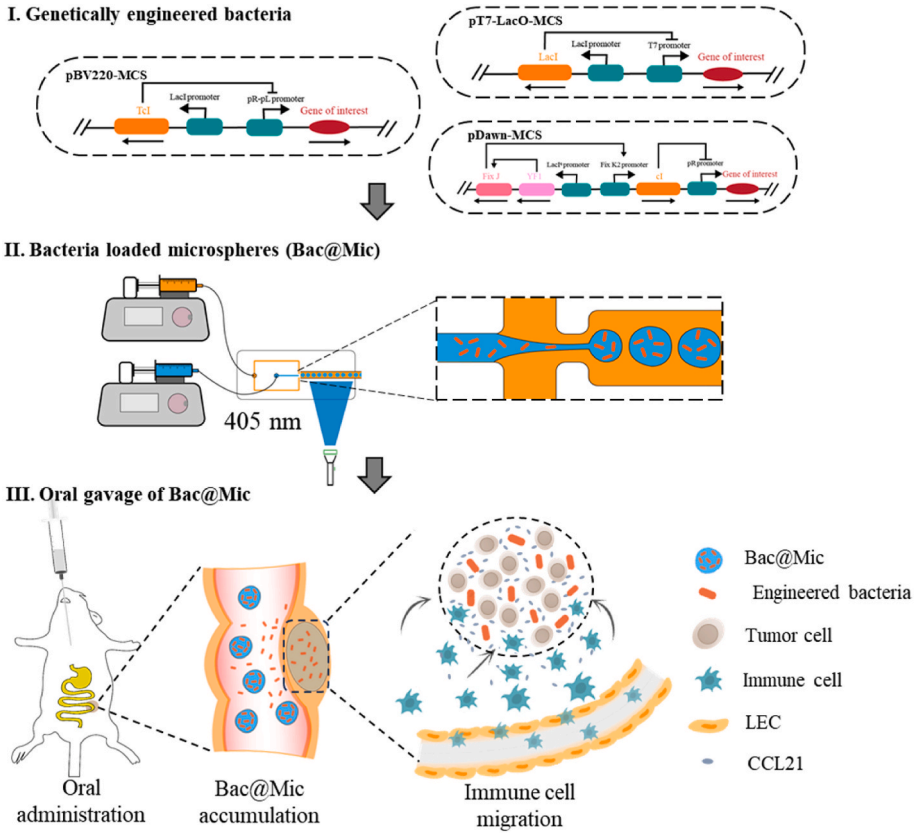

Scheme 1. Schematic illustration of genetically engineered bacteria-loaded microspheres for colon cancer therapy. Genetically engineered circuit in bacteria enables controlled expression of recombinant CCL21 (I). Preparation of bacteria-loaded microspheres (Bac@Mic) (II). Bac@Mic treatment induces colon cancer therapy. CCL21 secretion from Bac@Mic recruits $CD8^+$ and $CD4^+$ T cells to the tumor site, promoting immune response against cancer cells. LEC: lymphatic endothelial cell (III).

obtained from Thermo Fisher Scientific (Waltham, MA, USA). The gelatin and methacrylic anhydride were obtained from Aladdin Biochemical Technology (Shanghai, China). The plasmids including pDawn-mCherry (P1180) and pBV220 (P0367) were obtained from MiaoLingBio (Wuhan, China), and all the other plasmids used in this work were listed in Table S2. PCR amplification kit was obtained from Takara Biomedical Technology (Beijing, China) and cloning kit was purchased from Vazyme Biotechnology (Nanjing, China). The detailed sequence of the target protein was listed in Table S4 and the primers were listed in Table S3. The remaining necessary chemicals were sourced from commercial suppliers and were of analytical grade.

2.2. Animal experiment

Male C57BL/6 mice aged 6–8 weeks were procured from the Laboratory Animal Center of Zhengzhou University, Henan, China. All animal experiments were conducted under protocols approved by the Institutional Animal Care and Use Committee (IACUC) of Zhengzhou University (approval number: 2021-KY-0028)

2.3. Plasmid construction

The target gene encoding CCL21 was obtained from NCBI (Accession no.: CR450326.1). The encoding sequence was optimized for prokaryotic expression, and subsequently, the optimized cDNA sequence was synthesized by GENWIZ (Suzhou, China). The plasmid of pT7-Trx-CCL21 was constructed according to our previous work [16]. Briefly, the fragment CCL21 was sub-cloned into pET32a vector to prepare the IPTG induced Trx-CCL21 expression system. Similarly, PCR was employed to amplify the CCL21, Trx-CCL21, and mCherry gene fragments for sub-cloning into the pDawn and pBV220 vectors, respectively. This resulted in the creation of a target protein expression system that could be induced by blue light or a temperature of 42 °C. The constructed vectors were subsequently transformed into bacteria to generate the genetically engineered bacteria. These engineered bacteria were then stored at −80 °C for future utilization.

2.4. Expression of CCL21 and Trx-CCL21

The *E. coli* strains (Nissle 1917, obtained from GENWIZ, Suzhou, China) were cultivated in Luria Bertani (LB) medium, which contained 10 g/L tryptone, 5 g/L yeast extract and 10 g/L NaCl, followed by a constant shaking with 220 rpm at 37 °C. Once the culture reached an OD_{600} of 0.6–0.8 for the pT7-LacO expression system and 0.4–0.6 for the pDawn and pBV220 expression systems, the genetically engineered bacteria were subjected to treatment. This involved exposure to 1 mM IPTG, 470 nm blue light illumination for 30 min, or a 42 °C water bath for 30 min. Subsequently, they were further incubated at 37 °C with constant shaking at 220 rpm for 4 h. Following this incubation period, the Bacterial cells were harvested via centrifugation at 4000 rpm for 10 min, after which they were resuspended in lysis buffer (50 mM NaH_2PO_4, 300 mM NaCl, pH 8.0) with an equal volume. Then, sonicated until the solution became homogeneous and centrifuged at 12, 000 rpm for 15 min at 4 °C to obtain the soluble protein. The precipitation was dissolved in lysis buffer containing 8 M urea to obtain the inclusion body protein. The expression levels of the target proteins CCL21 and Trx-CCL21 were analyzed using 15 % and 10 % Sodium dodecyl sulfate polyacrylamide gel electrophoresis (SDS-PAGE), respectively.

2.5. Synthesis of GelMA

The synthesis of GelMA refers to the existing methods [30]. In detail, 5 g of gelatin (Aladdin Biochemical Technology, Shanghai, China) were dissolved in 50 mL PBS at 50 °C to obtain a 10 % (w/v) solution of gelatin. Afterwards, 5 mL of methacrylic anhydride (MA, Aladdin Biochemical Technology, Shanghai, China) were added to the gelatin solution with a rate of 0.5 mL/min. The gelatin solution was kept at 50 °C during the experiment process. The mixture was further stirred in dark for 3 h, followed by diluted with 250 mL warm PBS (50 °C). The mixtures were then dialyzed against Milli-Q water at 40 °C using a dialysis with a 12–14 kDa molecular weight cut-off (Beyotime Biotechnology, Shanghai, China) to remove salts and extra MA. The GelMA foam was obtained after freeze-drying and they were stored at −80 °C for further use.

2.6. Preparation of microspheres

Dissolved 0.5 g of GelMA foam in 5 mL Milli-Q water to obtain a 10 % (w/v) GelMA solution, and added 12.5 mg Lithium Phenyl (2, 4, 6-trimethylbenzoyl) phosphinate (LAP, Energy Chemical, Shanghai, China) into GelMA solution to form a mixed solution of 0.25 % (w/v) LAP in GelMA. The solution was kept in dark and used for preparation of microspheres. In detail, the solution mixed with genetically engineered bacteria at 5×10^9 CFU/mL was used as an internal phase liquid, and they were flowed out at a rate of 400 μL/h. The liquid paraffin with 1 % nonionic surfactants Span 80 (Aladdin Biochemical Technology, Shanghai, China) was served as external phase liquid and they were flowed out at a rate of 1250 μL/h. A uniform droplet could be formed at the junction of the two phases, caused by the different polarity between outer phase and inner phase. The GelMA microspheres were formed after exposing the droplets to blue light at 405 nm. Finally, the obtained Bac@Mic were washed with PBS three times and stored at 4 °C for further use.

2.7. Cell migration assay

The 4T1 cell line was used for cell migration analysis. Cells were harvested at a density of 3.0×10^4 per well and seeded into a 96-well plate. They were then starved overnight in culture medium containing 1 % FBS. Uniform scratch wounds were created using a WoundMaker (Essen BioScience). Following a wash with PBS, the culture medium from Bac@Mic (after induction for 6 h) was collected and added to each well. A control group was established using medium with wild type Bac@Mic culture. Migration distances were observed using the 10 × objective lens of the IncuCyte incubator (Essen BioScience) at 8-h intervals, and migration distance rates were quantified using ImageJ software.

2.8. Evaluation of Bac@Mic residence time in vivo

To detect the residence time of bacteria loaded microsphere *in vivo*, male C57BL/6 mice (three mice in each group) were used and administrated with PBS, Bac@Mic or naked bacteria by oral gavage. All the bacteria were genetically engineered for stable expression of mCherry. This allowed us to detect the fluorescent signal at the intestine site of mice. Therefore, the fluorescence and fluorescent intensity of mCherry from the intestine of mice was measured using the IVIS Lumina Imaging System (Xenogen Corporation, Hopkinto, MA) at the time point of 1, 24 and 48 h upon treatment. The image was analyzed using Living Image software (version 4.3.1).

2.9. Antitumor efficacy of Bac@Mic in colon cancer models

To construct the colon cancer models, mice were anesthetized and a small incision was made in the abdomen. The colon was exteriorized, and 2×10^6 MC38-Luc cells suspended in 50 μL volume of sterile saline were injected directly into the wall of the colon using a fine needle. After injection, the colon was repositioned inside the abdomen, and the incision was closed with sutures. After 7 days, mice were randomly assigned to different groups and received oral administration of PBS, blank microspheres, blue light-induced cell microspheres, heat-induced cell microspheres, and IPTG-induced cell microspheres at 200 μL per mouse. Treatment was administered on days 7, 11, 15, and 19. Each

mouse received an intraperitoneal injection of 15 mg/mL D-luciferin (10 μL/g of body weight, D812647, Macklin) in Dulbecco's PBS (DPBS) and was subsequently anesthetized with 2 % isoflurane before undergoing bioluminescence imaging. Bioluminescence images of the mice were obtained using the IVIS Lumina Imaging System (Xenogen Corporation, Hopkinton, MA). Regions of interest were quantified using Living Image® 4.1 software, and the results were expressed as average radiance (p/sec/cm^2/sr).

2.10. Biological markers and histological analysis

After long-term treatments, the mice were euthanized, and serum-based markers for liver function, renal function, and hematological parameters were analyzed. The major organs, including heart, lungs, liver, spleen, and kidneys, were collected and preserved in a 4 % formalin solution (w/v) at 25 °C for 2 days. For histological examination, the fixed tissue samples underwent dehydration through a series of ethanol dilutions. Subsequently, the samples were embedded in paraffin and sectioned into 6 μm thick vertical cross-sections. Hematoxylin and Eosin (H&E) staining was then employed to visualize tissue structure and specific components on the micro-sections. The stained micro-sections were finally scrutinized under an optical microscope (Carl Zeiss, Germany) to evaluate histological characteristics.

2.11. Flow cytometry

The single-cell suspension was obtained from the tumor tissue. In details, the tumor tissue was diced into small fragments, then digested at 37 °C in DMEM containing 1 mg/mL of collagenase III and 10 % fetal bovine serum for 30 min. Subsequently, the suspension was passed through a 100-mesh steel sieve to eliminate any remaining undigested tissue. The suspension was then centrifuged at 2000 rpm for 5 min at 4 °C, the cells were resuspended in a staining buffer (1 % BSA solution), and centrifuged again, with the washing process being repeated twice. Following the removal of the supernatant, the cells were resuspended in 100 μL of staining buffer, flow cytometry antibodies were added in the recommended proportions, and the mixture was incubated in the dark at 4 °C for 30 min. The antibodies used for immune cell analysis were listed in Table S5. Following resuspension of the cells in an appropriate volume of staining buffer, detection was conducted using the CytoFlex LX Flow Cytometer. Subsequent data analysis was performed utilizing FlowJo V_10 software.

2.12. Real time PCR analysis

Total RNA was isolated from the tumor samples using RNA isolator Total Extraction Reagent (Vazyme; Nanjing, China; Catalog no. R401) according to the manufacturer's instructions. Subsequently, 1 μg of RNA was reverse transcribed into complementary DNA (cDNA) using HiScript III All-in-one RT Supermix (Vazyme, Catalog no. R333). Real-time polymerase chain reaction (RT-PCR) was performed on a Real-Time PCR Instrument (Applied Biosystems™ 7500) using Taq Pro Universal SYBR qPCR Master Mix (Vazyme, Catalog no. Q712) to determine the expression levels of target genes. The results were normalized to the expression of the housekeeping gene glyceraldehyde 3-phosphate dehydrogenase (GAPDH) and presented as relative mRNA levels using the standard ΔΔCt method. Triplicate samples were analyzed ($n = 3$).

2.13. Statistical analyses

Data were processed using GraphPad Prism version 8 (San Diego, CA, USA). All data generated from animals were presented as the mean ± standard deviation (SD) of values obtained from three or more experiments. Student's t-test was used to compare two groups, and a $p < 0.05$ was considered as significant difference.

3. Results

3.1. Construction of recombinant expression vectors

To construct inducible expression bacteria, we introduced three types of promoters, including the pT7-LacO, pBV220 and pDawn, to the bacterial expression vectors. The pT7-LacO promoter is composed of a *LacI* promoter to express the repressor LacI, which inhibit the activation of T7 promoter. When IPTG is present, the repressor LacI will be removed from Lac operator, thus initiating the target gene expression (Scheme 1A). We then cloned DNA fragment containing 5′-UTR of genes Trx-CCL21, CCL21 or mCherry into the expression site of pT7-LacO vector to produce IPTG inducible expression system (Figure S1 and Figure S2). In the same manner as describe above, the target genes were also cloned into the other two types of vectors (pBV220-MCS and pDawn-MCS) respectively (Figs. S3–S6). All the nucleotide sequence of synthetic target gene was further confirmed by DNA sequencing (Table S1). Additionally, the nucleotide sequence of the target gene was codon-optimized for its heterologous expression.

3.2. Controlled expression of recombinant CCL21

Controlled gene expression with promoters that respond to chemicals, heat and light is the most often used strategy for microbial cell-based therapy [31,32]. Therefore, we evaluated the solubility of the target protein expressed in bacteria, which was induced by IPTG, a temperature of 42 °C and blue light. To achieve this, all the recombinant plasmids were transformed into bacteria respectively. After inducible expression, the soluble and insoluble protein fraction were separated and analyzed using 12 % SDS-PAGE. The intensities of the target protein bands were measured using ImageJ software according to the integrated density of SDS-PAGE gels. The results demonstrated that CCL21 was successfully expressed in bacteria upon treatment with different inducers. The soluble expression level of CCL21 was highest in pT7-LacO vector, while very weak stained band in pBV220 and pDawn vector groups. Meanwhile, the higher expression level of Trx-CCL21 was also found in pT7-LacO vector, indicating that this vector is more suitable for soluble expression of exogenous proteins (Fig. 1A–B, D-E and G-H). We also evaluated the influence of Trx tag on the soluble expression of recombinant CCL21. In the group of pT7-LacO, the percentage of soluble expression form was increased from 37.7 ± 1.4 to 84.2 ± 0.8 (Fig. 1C). Meanwhile, the increase of target protein as soluble form was also observed in the expression vector of pBV220 and pDawn, which were increased from 14.4 ± 1.1 to 47.5 ± 0.3 and from 20.4 ± 1.1 to 39.0 ± 1.2 (Fig. 1F and I), respectively. From above results, it was indicated that Trx fusion tag had an enhancement effect on the soluble expression of CCL21 protein in all expressed vectors. Once being fused with Trx tag, the enhancement of soluble expression part of CCL21 showed a trend of pT7-LacO-Trx-CCL21 > pBV220-Trx-CCL21 > pDawn-Trx-CCL21.

3.3. In vitro assessment of the activity of Bac@Mic

The utilization of bacteria-based therapy is often hindered by the challenging *in vivo* environment, characterized by factors like digestive enzymes and strong acids [33]. We therefore developed a microbial cell factory through encapsulating engineered bacteria within GelMA microgels (Bac@Mic). We first assessed the inducible ability of bacteria by transforming them with recombinant plasmids pT7-LacO-mCherry, pBV220-mCherry, or pDawn-mCherry (Fig. S7). After 9 h of culture, the growth rates of the engineered bacteria carrying the different plasmids exhibited no significant differences among the groups (Fig. 2A). The engineered bacteria were then encapsulated within GelMA microgels to form Bac@Mic, with the resulting images presented in Fig. S8. The duration of bacterial storage within the microspheres was evaluated using bacteria expressing mCherry within the Bac@Mic system. The bacteria can migrate outward from the GelMA microspheres starting on

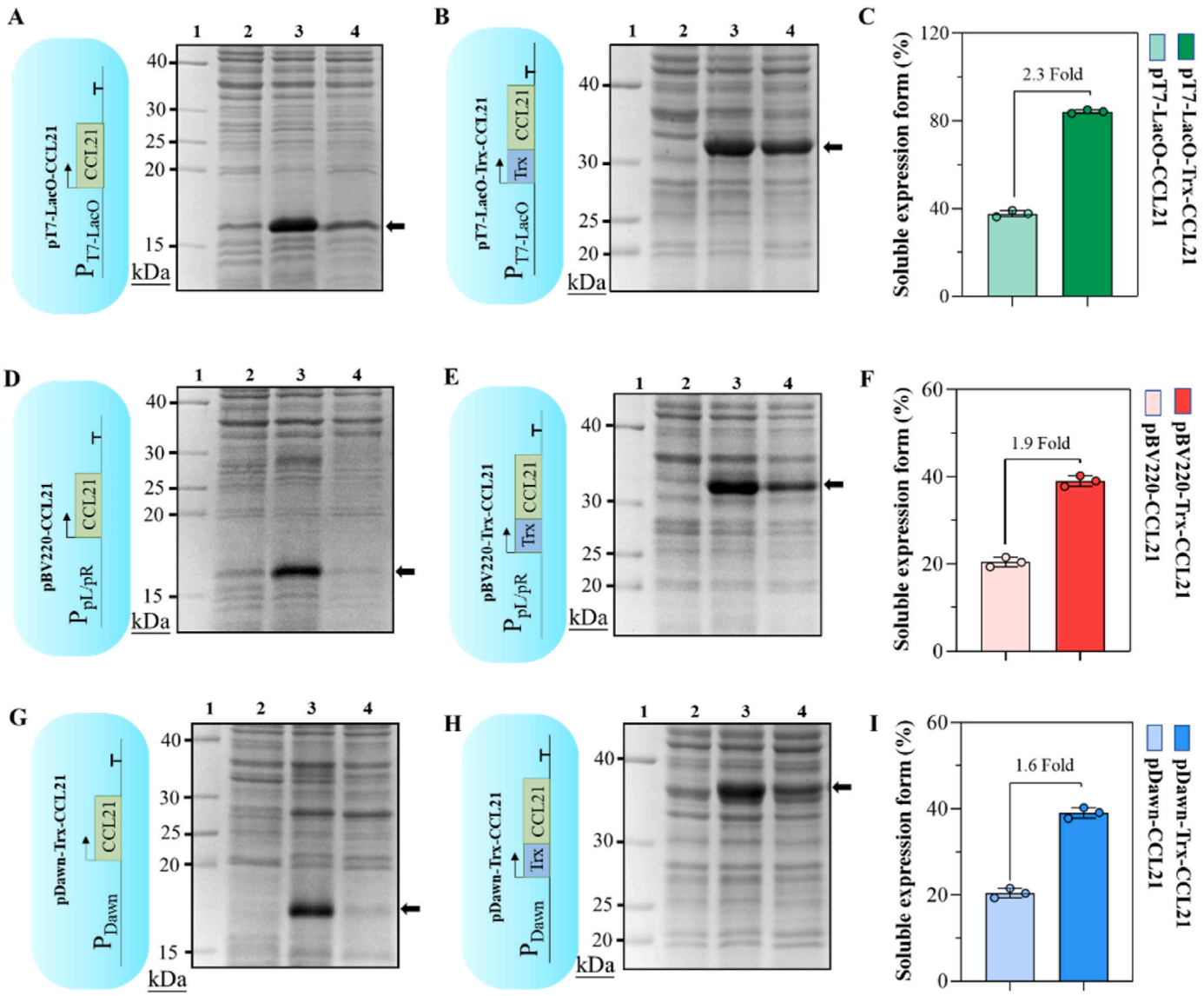

Fig. 1. Inducible expression of recombinant chemokines in bacteria. IPTG inducible expression of CCL21 (A) or Trx-CCL21 (B) visualized by SDS-PAGE. The ratio of soluble protein to total protein of CCL21 and Trx-CCL21 expressed under pT7-LacO promoter (C). Heat inducible expression of CCL21 (D) or Trx-CCL21 (E) visualized by SDS-PAGE. The ratio of soluble protein to total protein of CCL21 and Trx-CCL21 expressed under pBV220 promoter (F). Blue light inducible expression of CCL21 (G) or Trx-CCL21 (H) visualized by SDS-PAGE. The ratio of soluble protein to total protein of CCL21 and Trx-CCL21 expressed under pDawn promoter (I). The target protein was analyzed using image J software according to the integrated density of SDS-PAGE gels stained with Coomassie brilliant Blue (n = 3). Lane 1: protein molecular weight marker; Lane 2: Bacterial cells without induction; Lane 3: the total expression of target protein in bacterial cells; Lane 4: soluble form of the expression protein.

day 3 when cultured in LB medium (Fig. S9). The inducibility of Bac@Mic were further assessed at different time points using fluorescence microscopy (Fig. 2B), prior induction, mCherry signal kept silent at the basal level (0 min). Subsequent to treatment, the fluorescence intensity of mCherry exhibited a time-dependent response to the external inducers (Fig. 2C). The fluorescence was firstly detected in the bacteria-loaded microspheres after 90 min of exposure to blue light. In contrast, the groups treated with IPTG or 42 °C heat exhibited red fluorescence starting at 180 min after treatment. The results of the wound healing assay demonstrated that all three groups enhanced cell migration after 24 h (Fig. 2D and E). Additionally, a transwell experiment was conducted to further elucidate the recruitment effect of Bac@Mic on CCR7-positive cells, which showed increased migration following treatment with the three types of Bac@Mic (Fig. S10). These results suggest that the engineered Bac@Mic has the ability to recruit CCR7-positive cells.

3.4. Evaluation of residence time of Bac@Mic

Emerging evidence suggests that prolonging the residence time of exogenous bacteria *in vivo* is crucial for the effectiveness of live microbial therapy [34]. Here we conducted an examination of the *in vivo* stability of the microbial cell factory using genetically engineered bacteria transformed with a plasmid encoding mCherry. The mCherry expression in Bac@Mic remained stable throughout the experiment (Fig. 3A and B). Subsequently, healthy mice (C57BL/6) were orally administered with engineered Bac@Mic via gavage. The bacterial fluorescence was detected at 1, 24, and 48 h using an *in vivo* imaging system (IVIS) to observe the presence of engineered bacteria in live mice (Fig. 3C and D). The results showed a significant decrease in fluorescence of naked bacteria after 24 h of treatment, and the fluorescence were weakly detected after 48 h. In contrast, the microspheres significantly enhanced the *in vivo* longevity of the bacteria, as evidenced by

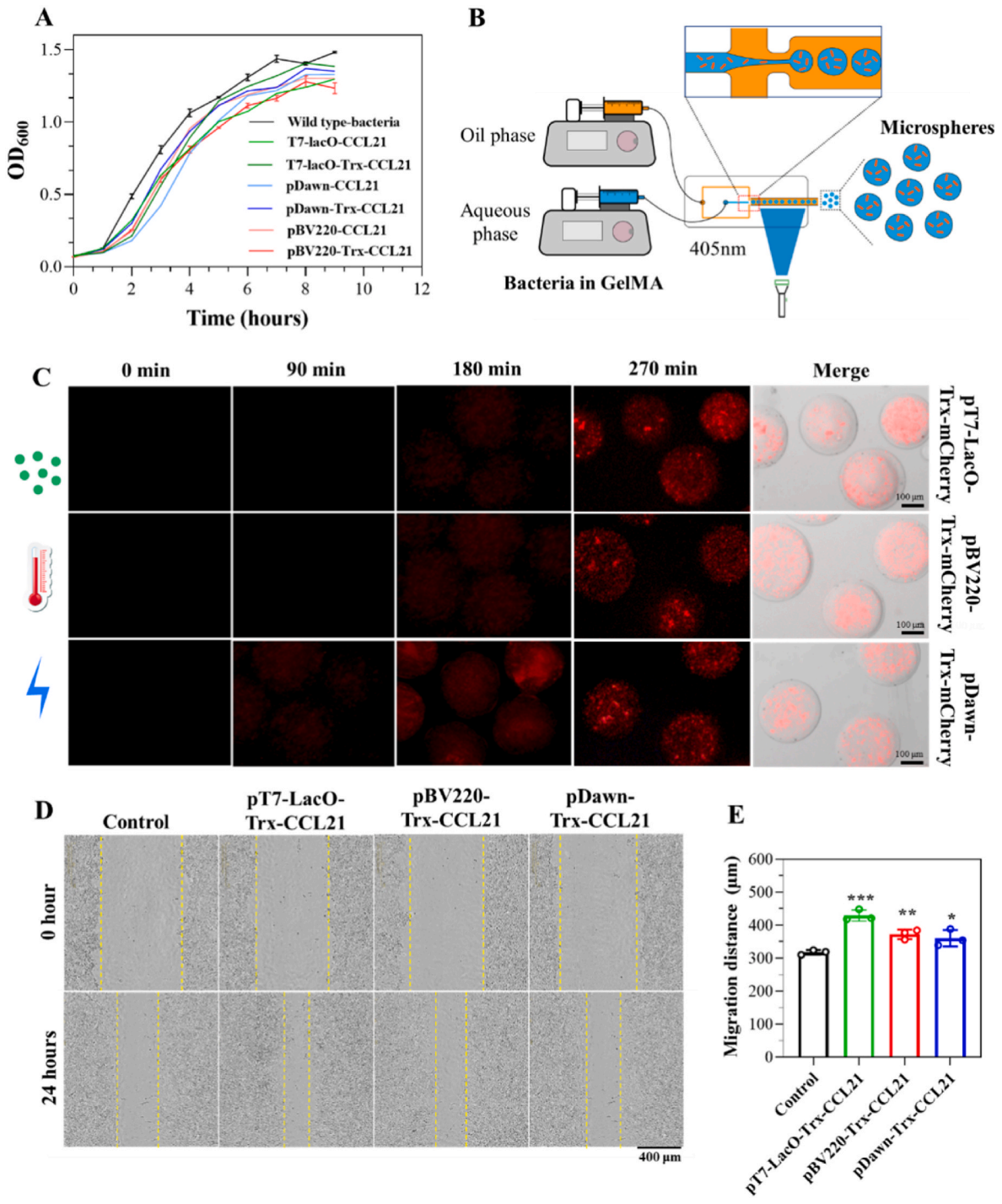

Fig. 2. Characterization of engineered Bac@Mic and its assessment of cell migration. (A) The growth curves of genetically engineered bacteria and those of wild-type bacteria. (B) Schematic showing the experimental procedure and time schedule used for inducible mCherry expression with IPTG, heating and blue light in engineered Bac@Mic. (C) Fluorescence image of time-dependent mCherry expression in the engineered Bac@Mic. (D) Migration of 4T1 cells upon treatment of engineered Bac@Mic for 0 or 24 h. (E) Quantitative analysis of cell migration distance upon treatment for 24 h. Data are presented as the mean ± SD, n = 6. ***$p < 0.001$; **$p < 0.01$; *$p < 0.05$.

their pronounced fluorescence in living mice, which persisted for up to 48 h after oral administration. After sacrificing the mice and harvesting the major organs, which were subsequently examined using an IVIS imaging system, the results revealed that the bacteria-loaded microspheres exhibited a markedly higher intensity in the intestinal regions compared to naked bacteria, demonstrating the superior retention capability of the microsphere delivery system (Fig. 3E). The biodistribution of different Bac@Mic was further investigated in colon tumor-bearing mice. The mice were euthanized, and their major organs were harvested. A slurry of the organs and tumor tissues was prepared and plated on Luria-Bertani (LB) plates to quantify colony-forming units (CFUs). The results indicated that bacteria were enriched and colonized in the tumor tissues, while their presence in the major organs was minimal within 48 h (Fig. S11). Additionally, we investigated the changes in CCL21 levels following Bac@Mic treatment using an ELISA assay. The results indicated that CCL21 levels were significantly higher

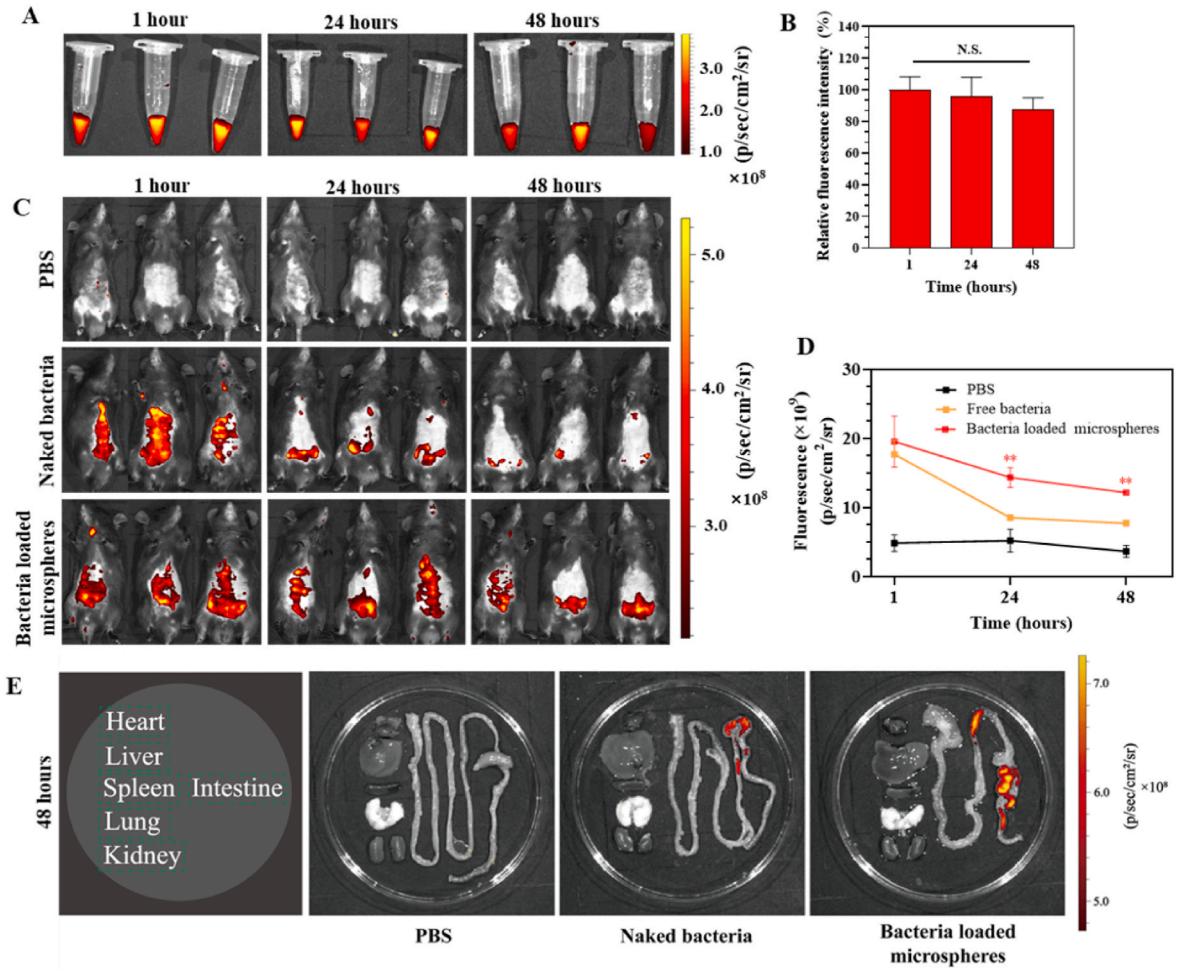

Fig. 3. Evaluation of residence time of engineered bacteria in mice gut. (A) IVIS images of living bacteria loaded microspheres in PBS at 1, 24 and 48 h respectively. (B) Relative mCherry fluorescent intensity of bacteria loaded microspheres *in vitro*. (C) IVIS images of mice treated with PBS, naked bacteria or bacteria loaded microspheres after the time points of 1, 24 and 48 h. (D) Quantification of mCherry fluorescent signals *in vivo*. Data are presented as the mean ± SD, n = 3. $^{**}p < 0.01$; N.S., no significant difference. (E) IVIS images of major organs following a 48-h treatment with PBS, naked bacteria, or bacteria-loaded microspheres.

in both *in vitro* and *in vivo* conditions compared to non-engineered bacteria, demonstrating the efficient release of CCL21 (Fig. S12).

3.5. Evaluation of in vivo anti-tumor efficacy of engineered Bac@Mic

Encouraged by the improved survival of engineered Bac@Mic in the mouse gut, we further investigated their potential as oral therapeutics for treatment of colon cancer in mice. The colon cancer model was constructed by directly injection of 2×10^6 MC38-Luc cells into the colon wall, and the treatment schedule outlined in Fig. 4A. Subsequently, we assessed the engineered anti-tumor efficacy of engineered Bac@Mic. As demonstrated in Fig. 4B, bioluminescence from MC38-Luc cancer cells rapidly increased in G1 and G2 mice. Compared with the G1 and G2 group, all the engineered Bac@Mic treatments led to suppressed tumor growth. Remarkably, bioluminescent cells were nearly eradicated in mice treated with engineered Bac@Mic up to 21 days post-tumor inoculation. Quantitative analysis of tumor bioluminescence further confirmed superior therapeutic efficacy of engineered Bac@Mic (Fig. 4C–E). The tumor intensity in mice was correlated with their survival: engineered Bac@Mic significantly prolonged survival, resulting in a 100 % survival rate after 50 days compared to the control groups (Fig. S13). The engineered Bac@Mic treatment resulted in elevated colon expression levels of IFN-γ, IL-6 and TNF-α (Fig. 4F–H), along with increased numbers of $CD4^+$ and $CD8^+$ T cells (Fig. 5A–Dand Figs. S14A and B). We further analyzed changes in immune cell, including natural killer (NK) cells, dendritic cells (DCs), central memory T cells (TCM), and regulatory T cells (Tregs), within the tumor microenvironment. The results demonstrated a significant increase in NK cells (Fig. 5E, F and Fig. S14C), DCs (Fig. 5G, H and Fig. S14D), and TCM (Fig. 5I, J and Fig. S14E) following treatment with engineered Bac@Mic. Additionally, the treatment disrupted the immunosuppressive nature of the tumor, leading to enhanced immune infiltration and a decrease in the proportion of regulatory T cells (Fig. 5K, L and Fig. S14F). These results suggest that engineered Bac@Mic effectively recruits immune cells, thereby enhancing the anti-tumor immune response. The biosafety of the Bac@Mic was preliminarily evaluated by measuring the weight loss of the mice and by pathological tissue analysis. The administration of Bac@Mic did not affect the body weights of the mice or key organs (Figure S15, Fig. 6 and Fig. 7).

4. Discussion

The advancement of precision medicine has emerged as a significant focus in healthcare policy in recent years [35,36], while traditional therapeutic approaches often fall short in meeting the requirements of precision medicine [37]. Furthermore, systemic drug administration may lead to uncontrollable and toxic side effects. Bacteria have been explored as microdevices for drug delivery due to their unique living characteristics, which allow them to transport macromolecular drugs through genetic engineering [38,39]. Furthermore, various therapeutics

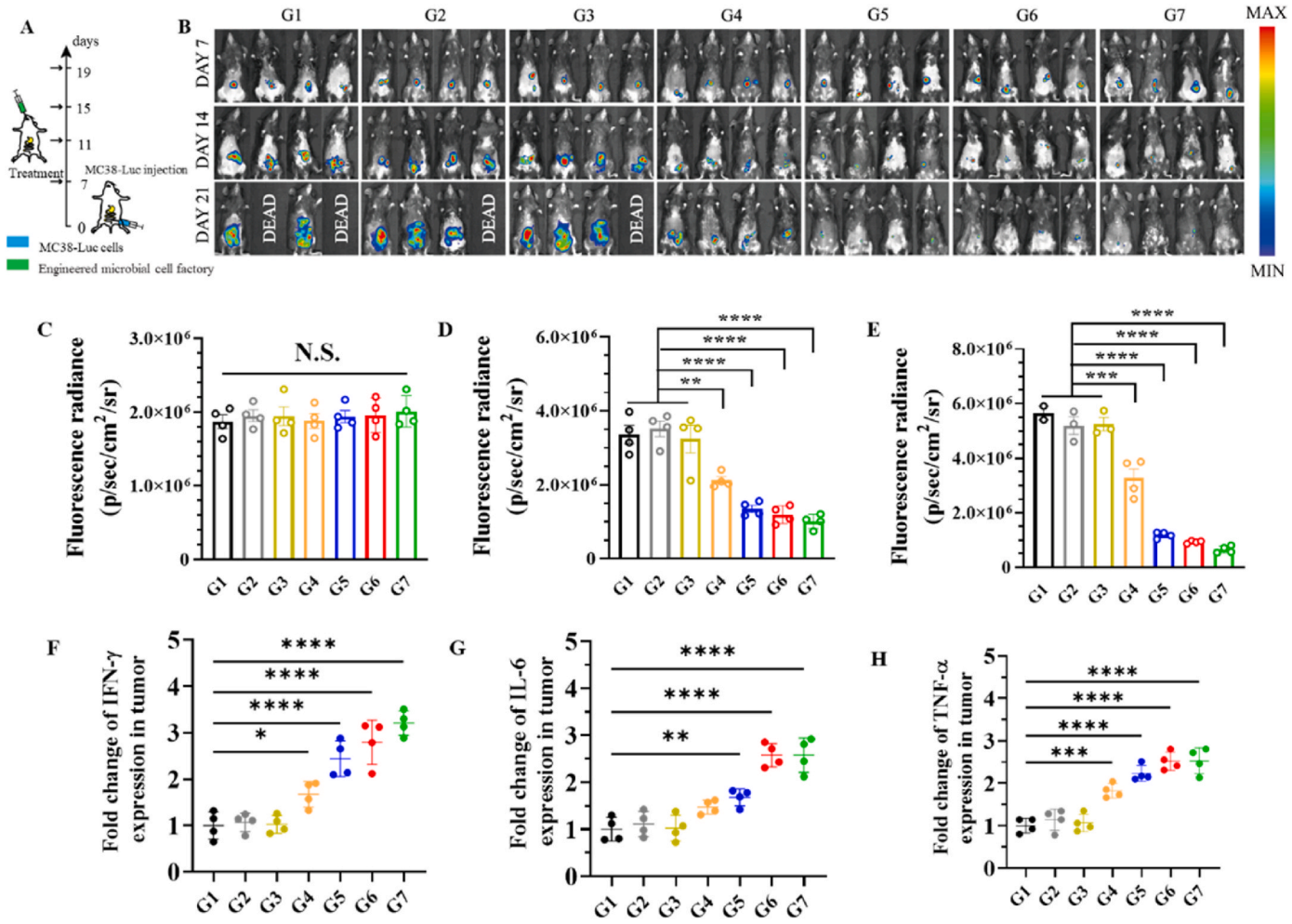

Fig. 4. ***In vivo*** **anti-tumor efficacy of engineered Bac@Mic in MC38-Luc tumor models.** (A) The schedule of antitumor efficacy study. (B) Serial *in vivo* bioluminescence imaging of MC38-Luc Tumors expressing luciferase after different treatments, n = 4. (C–E) Quantitative analysis of tumor bioluminescence intensity on days 7, 14, and 21. (F–H) Expression levels of IFN-γ, TNF-α, and IL-6 in tumors on day 21 following different treatments. G1: PBS; G2: Blank microsphere; G3: non-engineered bacteria@microgels; G4: Naked bacteria (IPTG induction); G5: Bac@Mic (Blue light induction); G6: Bac@Mic (Heat induction); G7: Bac@Mic (IPTG induction). Data are presented as the mean ± SD, n = 4. ****p < 0.0001; ***p < 0.001; **p < 0.01; *p < 0.05; N.S., no significant difference.

can be attached to bacteria via physicochemical modifications [40]. Harnessing their ability to colonize specific sites, such as disease sites, bacterial systems have been engineered to deliver drugs precisely and continuously to targeted locations. In contrast to traditional drug delivery systems, bacterial microdevices offer advantages such as in situ production of biologicals, prolonged colonization in the intestine, targeted delivery capability, and versatility in loading diverse drugs. On the other hand, advancements in synthetic biology and the increasing understanding of molecular disease mechanisms have facilitated the development of bacteria-engineered smart living therapeutics [41–43]. These innovations hold significant promise for treating human diseases [44–46].

In this present work, we engineered living bacteria to express therapeutic proteins in a controlled manner. To decrease the formation of infusion bodies (IBs) in bacteria, we used thioredoxin (Trx) as the fusion partner and cloned at N-terminal of the target protein. The different kinds of promoters, including pT7-LacO, pBV220, and pDawn, were designed and used to investigate the effects of different inducers on expression of CCL21 in bacteria. Our results demonstrated that Trx fusion tag can enhance the soluble expression form of CCL21 protein in all expressed vectors. Furthermore, our previous work has confirmed that Trx did not affect the functions of CCL21 [16]. As for the tree types of promoters, the engineered bacteria with the promoter of pT7-LacO can effectively produce soluble CCL21, nonetheless, the toxicity of IPTG might impact their clinical application. We further constructed the bacteria-loaded microspheres, followed by treated by different inducers, and we found that the engineered bacteria-loaded microspheres had a more rapid response to external blue light illumination. In general, optical control technology is a promising tool for precious regulation, while blue light illumination still has some limitations, such as its poor tissue penetration [47]. We additionally evaluated the viability of the bacteria-loaded microspheres *in vivo*. The stronger fluorescence observed in living mice suggests that the microspheres facilitated longer retention of bacteria in the intestine of mice. Finally, we investigated the anti-cancer efficacy of the three types of engineered Bac@Mic. The results demonstrated that all engineered Bac@Mic effectively suppressed tumor growth. However, no significant differences were observed in their effectiveness. The lack of a method for *in vivo* activation of the expression of recombinant CCL21 may have contributed to the uniform effectiveness observed among the engineered Bac@Mic types. Therefore, there is a pressing need to develop a strategy that can precisely control the release of CCL21, which requires further investigation to optimize therapeutic outcomes. Controlled release of chemokines can facilitate the penetration and persistence of T cells within the tumor, thus enhancing immune response against tumors. This strategy to prepare controlled microbial cell factory for chemokine production can provide important ideas to meet the application demands of precision medicine.

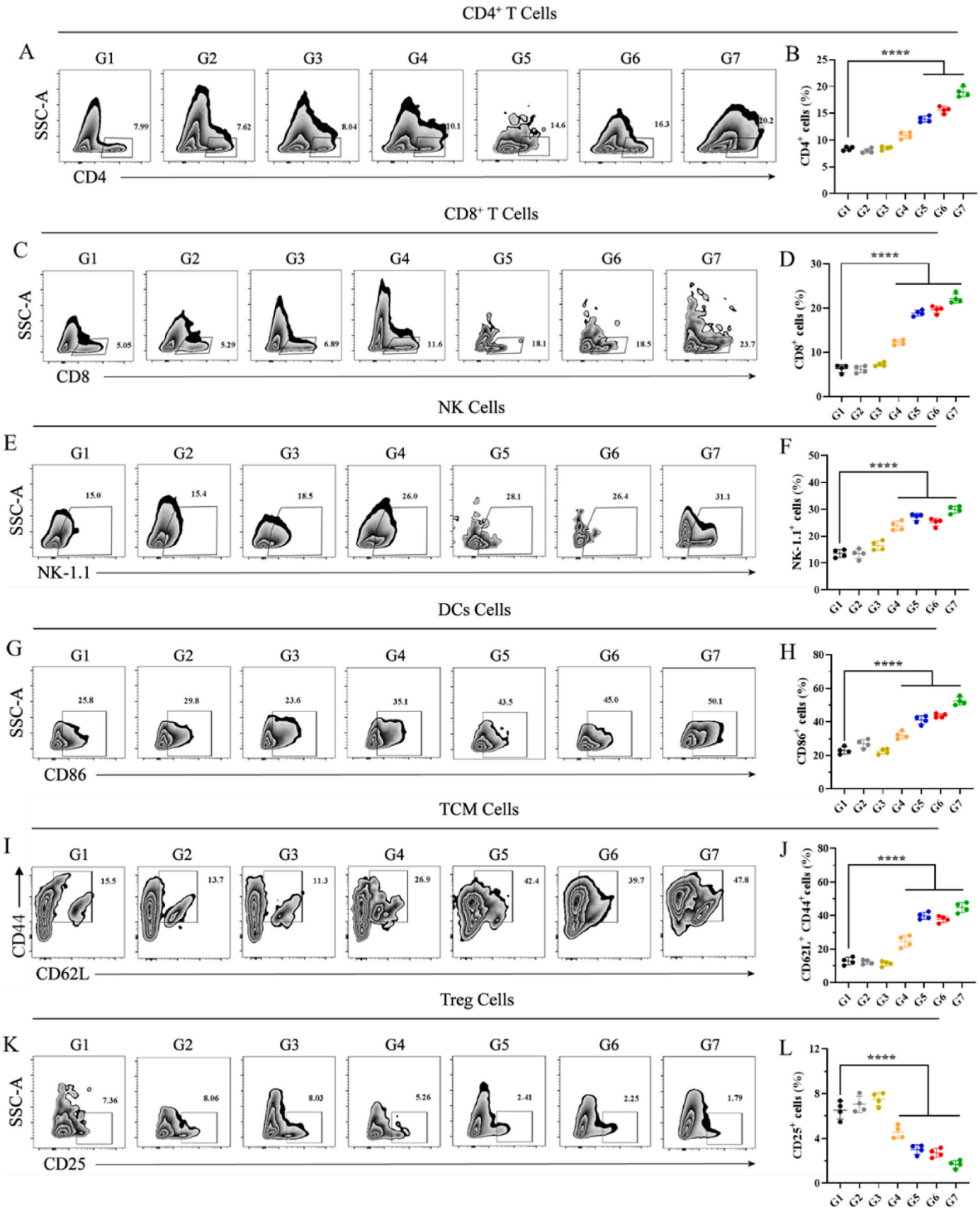

Fig. 5. ***In vivo*** **immune response of engineered Bac@Mic.** Representative flow cytometry images and statistical analysis of $CD4^+$ T cells (A, B), $CD8^+$ T cells (C, D), NK cells (E, F), DCs Cells (G, H), TCM Cells (I, J) and Treg Cells (K, L) in tumor. G1: PBS; G2: Blank microsphere; G3: Non-engineered bacteria@microgels; G4: Naked bacteria (IPTG induction); G5: Bac@Mic (Blue light induction); G6: Bac@Mic (Heat induction); G7: Bac@Mic (IPTG induction). Data are presented as the mean ± SD, n = 4. ****$p < 0.0001$.

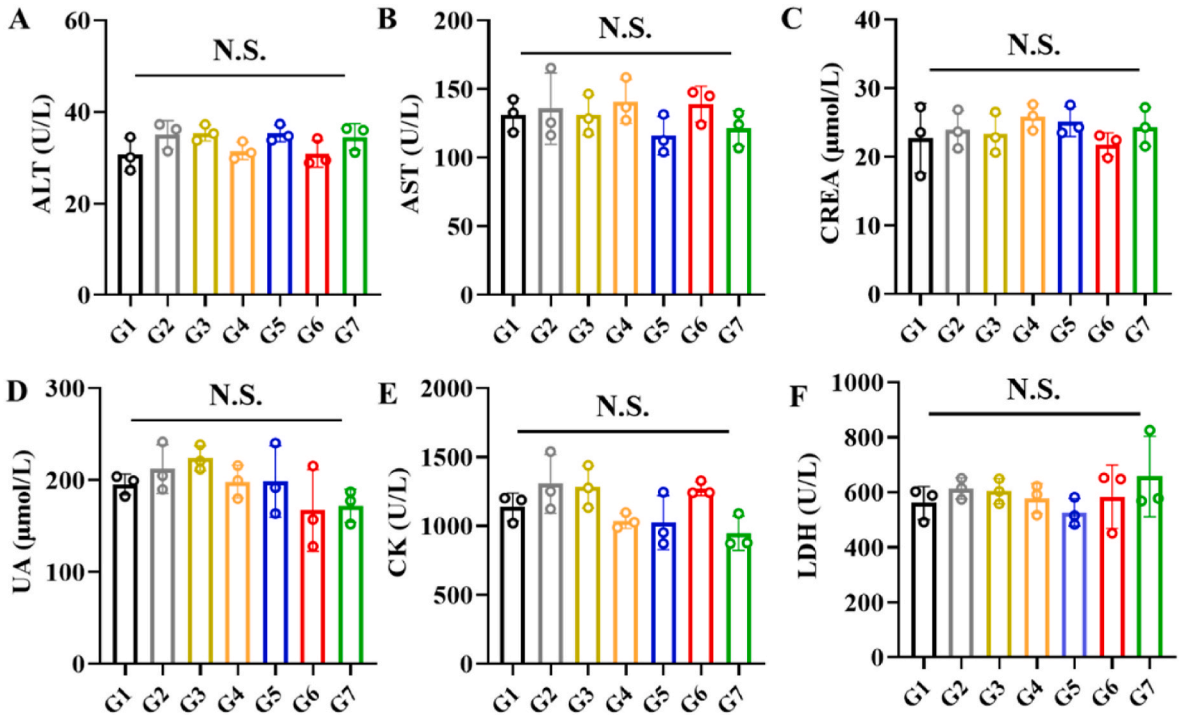

Fig. 6. The blood biochemical analysis of mice after different treatment. (A) ALT, alanine aminotransferase; (B) AST, aspartate transaminase; (C) CREA, creatinine; (D) UA, urine acid; (E) CK, creatine kinase; (F) LDH, lactate dehydrogenase. G1: PBS; G2: Blank microsphere; G3: Non-engineered bacteria@microgels; G4: Naked bacteria (IPTG induction); G5: Bac@Mic (Blue light induction); G6: Bac@Mic (Heat induction); G7: Bac@Mic (IPTG induction). Data are presented as the mean ± SD, n = 3. N.S., no significant difference.

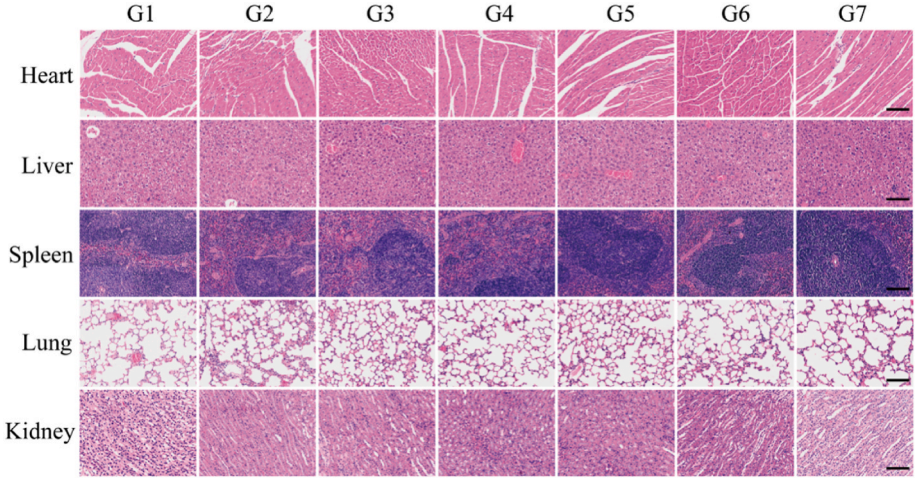

Fig. 7. H&E staining of the heart, liver, spleen, lung, and kidney obtained from mice after indicated treatments. G1: PBS; G2: Blank microsphere; G3: Non-engineered bacteria@microgels; G4: Naked bacteria (IPTG induction); G5: Bac@Mic (Blue light induction); G6: Bac@Mic (Heat induction); G7: Bac@Mic (IPTG induction). Scale bar: 100 μm.

5. Conclusion

This work reported a genetically engineered bacterial cell factory, which could be used for continuous production of chemokines in a controlled manner. We constructed three types of expression system, which could be controlled by IPTG, a temperature of 42 °C or blue light. As a comparison, the engineered bacteria had a more rapid response to external blue light illumination. Additionally, their soluble expression form of CCL21 could be enhanced by fusion protein tag Trx. The engineered bacteria were encapsulated within spherical gelatin methacryloyl (GelMA) microgels to create a microbial cell factory, which prolonged the residence time of bacteria in the intestines of mice, leading to effective suppression of tumor growth. Our research might offer a novel solution for the existing limitations in bacteria-based therapy.

CRediT authorship contribution statement

Yazhou Chen: Writing – review & editing, Supervision, Funding acquisition, Formal analysis, Conceptualization. **Kehan Cai:** Formal analysis, Data curation. **Hui Zhao:** Software, Methodology. **Wenshuai Li:** Project administration, Investigation. **Xiaofang Gao:** Methodology. **Yinzheng Fu:** Software, Resources. **Kyubae Lee:** Writing – review & editing. **SiTian Li:** Writing – original draft, Visualization, Project

administration, Investigation, Data curation. **Shengjie Yao:** Validation, Project administration. **Tao Chen:** Data curation, Conceptualization.

Availability of data and materials

The data supporting the findings of this study are available upon request from the corresponding authors.

Ethics approval and consent to participate

All animal experiments were conducted following protocols approved by the Institutional Animal Care and Use Committee (IACUC) of Zhengzhou University (Approval No. 2021-KY-0028).

Consent for publication

Not applicable.

Declaration of competing interest

The authors declare that they have no known competing financial interests or personal relationships that could have appeared to influence the work reported in this paper.

Acknowledgements

This work was financially supported by the International Post-doctoral Exchange Fellowship Program (Talent-Introduction Program, YJ20220182 to Yazhou Chen), and the High-level Talent International Training Project of Henan Province (Grant Nos. 22180001 to Yazhou Chen).

Appendix A. Supplementary data

Supplementary data to this article can be found online at https://doi.org/10.1016/j.mtbio.2024.101337.

Data availability

No data was used for the research described in the article.

References

[1] L. Tiberio, A. Del Prete, T. Schioppa, F. Sozio, D. Bosisio, S. Sozzani, Chemokine and chemotactic signals in dendritic cell migration, Cell. Mol. Immunol. 15 (4) (2018) 346–352.
[2] H. Xu, S. Lin, Z. Zhou, D. Li, X. Zhang, M. Yu, R. Zhao, Y. Wang, J. Qian, X. Li, B. Li, C. Wei, K. Chen, T. Yoshimura, J.M. Wang, J. Huang, New genetic and epigenetic insights into the chemokine system: the latest discoveries aiding progression toward precision medicine, Cell. Mol. Immunol. 20 (7) (2023) 739–776.
[3] N. Nagarsheth, M.S. Wicha, W. Zou, Chemokines in the cancer microenvironment and their relevance in cancer immunotherapy, Nat. Rev. Immunol. 17 (9) (2017) 559–572.
[4] N. Karin, Chemokines and cancer: new immune checkpoints for cancer therapy, Curr. Opin. Immunol. 51 (2018) 140–145.
[5] N. Aziz, R. Detels, J.J. Quint, Q. Li, D. Gjertson, A.W. Butch, Stability of cytokines, chemokines and soluble activation markers in unprocessed blood stored under different conditions, Cytokine 84 (2016) 17–24.
[6] N. Karin, H. Razon, Chemokines beyond chemo-attraction: CXCL10 and its significant role in cancer and autoimmunity, Cytokine 109 (2018) 24–28.
[7] D.-H. Nguyen, A. Chong, Y. Hong, J.-J. Min, Bioengineering of bacteria for cancer immunotherapy, Nat. Commun. 14 (1) (2023) 3553.
[8] S. Zhou, C. Gravekamp, D. Bermudes, K. Liu, Tumour-targeting bacteria engineered to fight cancer, Nat. Rev. Cancer 18 (12) (2018) 727–743.
[9] X. Huang, J. Pan, F. Xu, B. Shao, Y. Wang, X. Guo, S. Zhou, Bacteria-based cancer immunotherapy, Adv. Sci. 8 (7) (2021) 2003572.
[10] D.H. Nguyen, A. Chong, Y. Hong, J.J. Min, Bioengineering of bacteria for cancer immunotherapy, Nat. Commun. 14 (1) (2023) 3553.
[11] H. Pan, L. Li, G. Pang, C. Han, B. Liu, Y. Zhang, Y. Shen, T. Sun, J. Liu, J. Chang, H. Wang, Engineered NIR light-responsive bacteria as anti-tumor agent for targeted and precise cancer therapy, Chem. Eng. J. 426 (2021) 130842.
[12] H. Chen, Y. Li, Y. Wang, P. Ning, Y. Shen, X. Wei, Q. Feng, Y. Liu, Z. Li, C. Xu, S. Huang, C. Deng, P. Wang, Y. Cheng, An engineered bacteria-hybrid microrobot with the magnetothermal bioswitch for remotely collective perception and imaging-guided cancer treatment, ACS Nano 16 (4) (2022) 6118–6133.
[13] S.H.-N. Joshi, C. Yong, A. Gyorgy, Inducible plasmid copy number control for synthetic biology in commonly used E. coli strains, Nat. Commun. 13 (1) (2022) 6691.
[14] M.H. Abedi, M.S. Yao, D.R. Mittelstein, A. Bar-Zion, M.B. Swift, A. Lee-Gosselin, P. Barturen-Larrea, M.T. Buss, M.G. Shapiro, Ultrasound-controllable engineered bacteria for cancer immunotherapy, Nat. Commun. 13 (1) (2022) 1585.
[15] J.R. Newman, C. Fuqua, Broad-host-range expression vectors that carry the l-arabinose-inducible Escherichia coli araBAD promoter and the araC regulator, Gene 227 (2) (1999) 197–203.
[16] S. Li, Y. Wang, H. Jiang, Y. Bai, T. Chen, M. Chen, M. Ma, S. Yang, Y. Wu, C. Shi, F. Wang, Y. Chen, Display of CCL21 on cancer cell membrane through genetic modification using a pH low insertion peptide, Int. J. Biol. Macromol. 240 (2023) 124324.
[17] X. Zhang, G. Pang, T. Sun, X. Liu, H. Pan, Y. Zhang, J. Liu, J. Chang, H. Wang, D. Liu, A red light-controlled probiotic bio-system for in-situ gut-brain axis regulation, Biomaterials 294 (2023) 122005.
[18] P. Jayaraman, K. Devarajan, T.K. Chua, H. Zhang, E. Gunawan, C.L. Poh, Blue light-mediated transcriptional activation and repression of gene expression in bacteria, Nucleic Acids Res. 44 (14) (2016) 6994–7005.
[19] X. Ma, X. Liang, Y. Li, Q. Feng, K. Cheng, N. Ma, F. Zhu, X. Guo, Y. Yue, G. Liu, T. Zhang, J. Liang, L. Ren, X. Zhao, G. Nie, Modular-designed engineered bacteria for precision tumor immunotherapy via spatiotemporal manipulation by magnetic field, Nat. Commun. 14 (1) (2023) 1606.
[20] Y. Chen, M. Du, Z. Yuan, Z. Chen, F. Yan, Spatiotemporal control of engineered bacteria to express interferon-γ by focused ultrasound for tumor immunotherapy, Nat. Commun. 13 (1) (2022) 4468.
[21] S. Chowdhury, S. Castro, C. Coker, T.E. Hinchliffe, N. Arpaia, T. Danino, Programmable bacteria induce durable tumor regression and systemic antitumor immunity, Nat. Med. 25 (7) (2019) 1057–1063.
[22] N. Jiang, K. Zhao, C. Liu, X. Zhu, X. Huang, L. Yang, X. Yi, Y. Zhuang, B. Ye, J. Qian, J. Huang, Tumor microenvironment responsive multifunctional smart living materials based on engineered bacteria for inducing macrophage polarization to enhance tumor immunotherapy, Chem. Eng. J. 488 (2024) 150820.
[23] P. Singhvi, A. Saneja, S. Srichandan, A.K. Panda, Bacterial inclusion bodies: a treasure trove of bioactive proteins, Trends Biotechnol. 38 (5) (2020) 474–486.
[24] N.C. Tang, J.C. Su, Y. Shmidov, G. Kelly, S. Deshpande, P. Sirohi, N. Peterson, A. Chilkoti, Synthetic intrinsically disordered protein fusion tags that enhance protein solubility, Nat. Commun. 15 (1) (2024) 3727.
[25] E. García-Fruitós, E. Vázquez, C. Díez-Gil, J.L. Corchero, J. Seras-Franzoso, I. Ratera, J. Veciana, A. Villaverde, Bacterial inclusion bodies: making gold from waste, Trends Biotechnol. 30 (2) (2012) 65–70.
[26] C. Mastini, M. Campisi, E. Patrucco, G. Mura, A. Ferreira, C. Costa, C. Ambrogio, G. Germena, C. Martinengo, S. Peola, I. Mota, E. Vissio, L. Molinaro, M. Arigoni, M. Olivero, R. Calogero, N. Prokoph, F. Tabbò, B. Shoji, L. Brugieres, B. Geoerger, S.D. Turner, C. Cuesta-Mateos, D. D'Aliberti, L. Mologni, R. Piazza, C. Gambacorti-Passerini, G.G. Inghirami, V. Chiono, R.D. Kamm, E. Hirsch, R. Koch, D. M. Weinstock, J.C. Aster, C. Voena, R. Chiarle, Targeting CCR7-PI3Kγ overcomes resistance to tyrosine kinase inhibitors in ALK-rearranged lymphoma, Sci. Transl. Med. 15 (702) (2023) eabo3826.
[27] A. Ciechanowska, J. Mika, CC chemokine family members' modulation as a novel approach for treating central nervous system and peripheral nervous system injury-A review of clinical and experimental findings, Int. J. Mol. Sci. 25 (7) (2024) 3788.
[28] A. Salem, M. Alotaibi, R. Mroueh, H.A. Basheer, K. Afarinkia, CCR7 as a therapeutic target in Cancer, Biochimica et biophysica acta, Reviews on cancer 1875 (1) (2021) 188499.
[29] L. Han, L. Zhang, CCL21/CCR7 axis as a therapeutic target for autoimmune diseases, Int. Immunopharm. 121 (2023) 110431.
[30] X. Li, J. Zhang, N. Kawazoe, G. Chen, Fabrication of highly crosslinked gelatin hydrogel and its influence on chondrocyte proliferation and phenotype, Polymers 9 (8) (2017) 309.
[31] Z. Li, Y. Wang, J. Liu, P. Rawding, J. Bu, S. Hong, Q. Hu, Chemically and biologically engineered bacteria-based delivery systems for emerging diagnosis and advanced therapy, Adv. Mater. 33 (38) (2021) 2102580.
[32] H. Pan, T. Sun, M. Cui, N. Ma, C. Yang, J. Liu, G. Pang, B. Liu, L. Li, X. Zhang, W. Zhang, J. Chang, H. Wang, Light-sensitive lactococcus lactis for microbe–gut–brain Axis regulating via upconversion optogenetic micro-nano system, ACS Nano 16 (4) (2022) 6049–6063.
[33] X. Yang, W. Nie, C. Wang, Z. Fang, L. Shang, Microfluidic-based multifunctional microspheres for enhanced oral co-delivery of probiotics and postbiotics, Biomaterials 308 (2024) 122564.
[34] X. Yang, J. Yang, Z. Ye, G. Zhang, W. Nie, H. Cheng, M. Peng, K. Zhang, J. Liu, Z. Zhang, J. Shi, Physiologically inspired mucin coated Escherichia coli nissle 1917 enhances biotherapy by regulating the pathological microenvironment to improve intestinal colonization, ACS Nano 16 (3) (2022) 4041–4058.
[35] X.-P. Duan, B.-D. Qin, X.-D. Jiao, K. Liu, Z. Wang, Y.-S. Zang, New clinical trial design in precision medicine: discovery, development and direction, Signal Transduct. Targeted Ther. 9 (1) (2024) 57.
[36] W. Abbaoui, S. Retal, B. El Bhiri, N. Kharmoum, S. Ziti, Towards revolutionizing precision healthcare: a systematic literature review of artificial intelligence methods in precision medicine, Inform. Med. Unlocked 46 (2024) 101475.
[37] E.A. Ashley, Towards precision medicine, Nat. Rev. Genet. 17 (9) (2016) 507–522.
[38] T. Gao, L. Niu, X. Wu, D. Dai, Y. Zhou, M. Liu, K. Wu, Y. Yu, N. Guan, H. Ye, Sonogenetics-controlled synthetic designer cells for cancer therapy in tumor mouse models, Cell Reports Medicine 5 (5) (2024) 101513.

[39] T.M. Savage, R.L. Vincent, S.S. Rae, L.H. Huang, A. Ahn, K. Pu, F. Li, K. de Los Santos-Alexis, C. Coker, T. Danino, N. Arpaia, Chemokines expressed by engineered bacteria recruit and orchestrate antitumor immunity, Sci. Adv. 9 (10) (2023) eadc9436.
[40] L. Zhu, T. Yu, W. Wang, T. Xu, W. Geng, N. Li, X. Zan, Responsively degradable nanoarmor-assisted super resistance and stable colonization of probiotics for enhanced inflammation-targeted delivery, Adv. Mater. 36 (18) (2024) 2308728.
[41] D.E. Cameron, C.J. Bashor, J.J. Collins, A brief history of synthetic biology, Nat. Rev. Microbiol. 12 (5) (2014) 381–390.
[42] V. Chubukov, A. Mukhopadhyay, C.J. Petzold, J.D. Keasling, H.G. Martín, Synthetic and systems biology for microbial production of commodity chemicals, NPJ. Sys. Biol. Appl. 2 (1) (2016) 16009.
[43] R. Pasupuleti, F. Rosato, D. Kolanovic, O.N. Makshakova, W. Römer, B. Wiltschi, Genetic code expansion in E. coli enables production of a functional 'ready-to-click' T cell receptor-specific scFv, N. Biotech. 76 (2023) 127–137.
[44] A. Cubillos-Ruiz, T. Guo, A. Sokolovska, P.F. Miller, J.J. Collins, T.K. Lu, J.M. Lora, Engineering living therapeutics with synthetic biology, Nat. Rev. Drug Discov. 20 (12) (2021) 941–960.
[45] R. Omer, M.Z. Mohsin, A. Mohsin, B.S. Mushtaq, X. Huang, M. Guo, Y. Zhuang, J. Huang, Engineered bacteria-based living materials for biotherapeutic applications, Front. Bioeng. Biotechnol. 10 (2022) 870675.
[46] A.K. Yanamandra, S. Bhusari, A. del Campo, S. Sankaran, B. Qu, In vitro evaluation of immune responses to bacterial hydrogels for the development of living therapeutic materials, Biomater. Adv. (2023) 213554.
[47] N. Guan, X. Gao, H. Ye, Engineering of optogenetic devices for biomedical applications in mammalian synthetic biology, Engineering Biology 6 (2–3) (2022) 35–49.